# Distinctive plume formation in atmospheric Ar and He plasmas in microwave frequency band and suitability for biomedical applications

H. Wk. Lee, S. K. Kang, I. H. Won, H. Y. Kim, H. C. Kwon, J. Y. Sim, and J. K. Lee

Citation: Physics of Plasmas (1994-present) **20**, 123506 (2013); doi: 10.1063/1.4841295
View online: http://dx.doi.org/10.1063/1.4841295
View Table of Contents: http://scitation.aip.org/content/aip/journal/pop/20/12?ver=pdfcov
Published by the AIP Publishing



# Distinctive plume formation in atmospheric Ar and He plasmas in microwave frequency band and suitability for biomedical applications

H. Wk. Lee, S. K. Kang, I. H. Won, H. Y. Kim, H. C. Kwon, J. Y. Sim,[a] and J. K. Lee[b]
*Department of Electrical Engineering, Pohang University of Science and Technology, Pohang 790-784, South Korea*

(Received 12 June 2013; accepted 22 November 2013; published online 10 December 2013)

Distinctive discharge formation in atmospheric Ar and He plasmas was observed in the microwave frequency band using coaxial transmission line resonators. Ar plasmas formed a plasma plume whereas He formed only confined plasmas. As the frequency increased from 0.9 GHz to 2.45 GHz, the Ar plasma exhibited contraction and filamentation, and the He plasmas were constricted. Various powers and gas flow rates were applied to identify the effect of the electric field and gas flow rate on plasma plume formation. The He plasmas were more strongly affected by the electric field than the Ar plasmas. The breakdown and sustain powers yielded opposite results from those for low-frequency plasmas (~kHz). The phenomena could be explained by a change in the dominant ionization process with increasing frequency. Penning ionization and the contribution of secondary electrons in sheath region reduced as the frequency increased, leading to less efficient ionization of He because its ionization and excitation energies are higher than those of Ar. The emission spectra showed an increase in the NO and $N_2$ second positive band in both the Ar and He plasmas with increasing frequency whereas the hydroxyl radical and atomic O peaks did not increase with increasing frequency but were highest at particular frequencies. Further, the frequency effect of properties such as the plasma impedance, electron density, and device efficiency were presented. The study is expected to be helpful for determining the optimal conditions of plasma systems for biomedical applications. © *2013 AIP Publishing LLC*. [http://dx.doi.org/10.1063/1.4841295]

## I. INTRODUCTION

Microwave-excited plasmas (>0.5 GHz) have several advantages over low-frequency plasmas (~kHz): high density of electron and reactive species, low breakdown power, and long electrode lifetime.[1–4] These advantages present excellent opportunities for using microwave-excited plasmas in emerging application fields in surface processing and biomedicine.[1,5] Especially for soft biomedical applications, coaxial transmission line resonator (CTLR) has shown the highest potential because it has the outstanding advantages of low power requirements, low-temperature operation, and operation at atmospheric pressure.[3]

Extensive research has been performed to observe the distinct characteristics of microwave plasmas. Radial contraction and filamentation were found in microwave-excited argon plasma.[6,7] The $\gamma$–$\alpha$ mode transition with changing frequency has been reported.[8–10] The discharge properties for various gas compositions, i.e., the discharge formation, breakdown voltage, and portion of reactive species, were also found to differ greatly from those of lower-frequency plasmas.[4] Low-frequency (~kHz) Ar and He plasmas exhibited similar plume formation although He plasma formed a longer and more stable plasma plume. Dominant ionization processes for sustaining plasmas are known to be stepwise ionization for Ar plasmas and Penning ionization for He plasmas.[11–14] $N_2$ has important role through Penning ionization process especially in He plasma because of high ionization and excitation energy levels of He. On the other hand, Naidis *et al*. reported the importance of He metastable species, ions, and direct impact ionization in DC nanopulsed He plasma.[15,16] Although further research is required, Penning ionization process is still important in He plasmas.[17,18] In the aspect of biomedical applications, He plasmas were favorable because of low breakdown voltage and higher portion of reactive species than Ar plasmas at low frequency.[4] He plasmas have more safety in electrical shock and gas temperature than Ar plasmas in low frequency systems.

Because the operating frequency is an important factor in the discharge characteristics, detailed observations of these characteristics are still required for the various microwave frequency bands. However, changing the operating frequency to observe its effects on the characteristics is not straightforward for microwave plasma systems. The optimal frequency for power transfer to plasma is fixed for a given resonator geometry because a microwave plasma utilizes resonance in the waveguide.[1,3,19,22] A conventional matching scheme based on transmission line theory can be used; however, failure eventually occurs when matching for operation over a wide frequency range. Thus, numerical analysis has been used to observe the effect of the frequency on microwave plasmas, and experimental results are still required.[8,20,21] In this paper, we present the discharge characteristics of CTLRs in three microwave frequency bands: 0.9, 1.4, and 2.45 GHz. The CTLRs have same geometry except their length for reasonable observation of discharge characteristics in microwave band. Plume formation, the emission

[a]Electronic mail: jysim@postech.ac.kr.
[b]Electronic mail: jkl@postech.ac.kr. Fax: 82-54-279-2903.

 

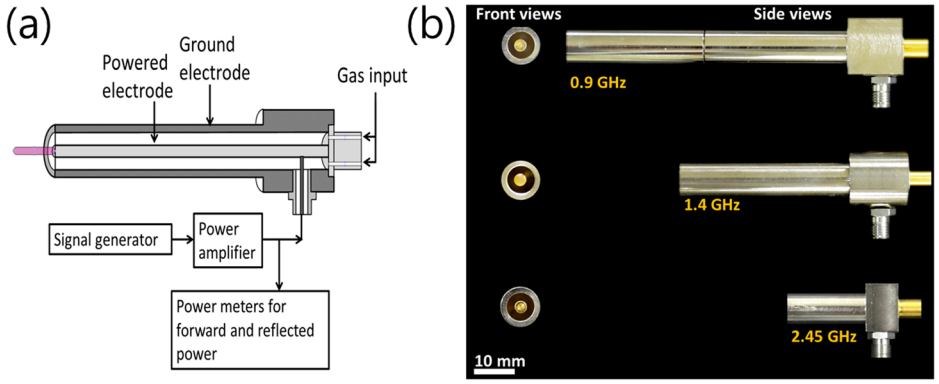


FIG. 1. (a) Cross-sectional diagram of CTLR structure and experimental setup. (b) Front and side views of 0.9-, 1.4-, and 2.45-GHz microwave plasma generators.

spectra, and the breakdown and sustain powers for sustaining the plasma will be investigated, and possible mechanisms for the distinctive characteristics will be presented.

## II. MATERIALS AND METHODS

### A. Description of plasma devices

Three devices based on CTLRs were designed for resonance frequencies of 0.9, 1.4, and 2.45 GHz.[3] The resonance of the implemented CTLRs occurred at approximately 0.88, 1.3625, and 2.365 GHz, respectively; however, we refer to 0.9-, 1.4-, and 2.45-GHz operation for simplicity. Without extra matching networks, matching can be obtained by optimally setting the location of the power feeding point, which reduces the size for hand-held use.[3] The devices have a shorted end at one side and an open end at the opposite side of the coaxial transmission line (Figure 1(a)). The diameter of the inner electrode is 3 mm, and the inner radius of the outer electrode is 7 mm. The total length of each device is approximately one-quarter of the wavelength of the resonance frequency. At the resonance frequency, the electric field (E-field) of the standing wave becomes the maximum at the open end, where plasma is generated. The devices have a pencil-shaped body 10 mm in diameter, and their lengths are about 85, 55, and 30 mm for 0.9, 1.4, and 2.45 GHz, respectively (Figure 1(b)). Gas is supplied through two 1-mm-diameter holes at the shorted end. The effect of the holes on the characteristics is negligible because their diameters are sufficiently small compared to the wavelengths.

The E-field shows a roughly uniform distribution on the cross section of the inner electrode (Figure 2(a)) whereas the edge of the cross section has the strongest E-field (Figure 2(b)). The E-field distribution and E-field vectors were calculated using High frequency structural simulator (HFSS, Ansoft). The matching performance was estimated using the $S_{11}$ parameter measured by a network analyzer (E5061B, Agilent). $S_{11}$ was around −18 dB at the resonance frequencies for the three devices before plasma ignition.

### B. Experimental setup

An RF signal generator (N1518A, Agilent) was connected to the resonators through a 46-dB power amplifier (RUM15040-01, RFHIC). The forward and reflected powers were measured by RF power meters (EPM441A, HP) (Figure 1(a)). Because the Ar and He plasmas have different minimum sustain powers, which also depend on the operating frequency, powers about 30% higher than the minimum sustain power at 2.45 GHz were selected for stable operation at all the frequencies; these were 5 W for the Ar plasmas and 15 W for the He plasmas. At the same 15 W power, Ar plasma exhibited different discharge formation phases with regular operation at 1.4 and 2.45 GHz; therefore, we were forced to select different operation powers for Ar and He. The gas flow rate was fixed at 4 standard liters per minute (slm) for the two gases and was measured by gas flow meters (KOFLOC). The Ar and He plasmas were generated in ambient air. A digital single-lens reflex camera (D7000, Nikon)

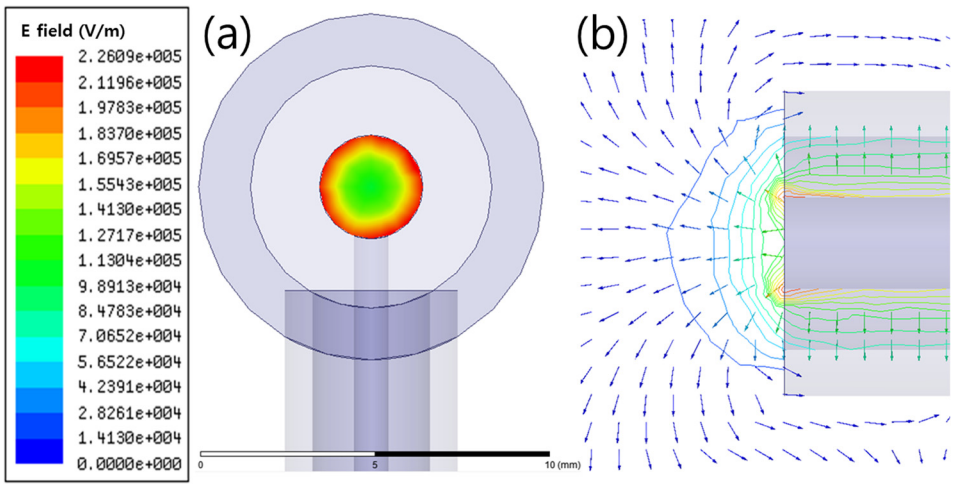


FIG. 2. (a) Electric field distribution of the inner electrode at open end, and (b) side views of vectors and electric field distribution of 0.9-GHz device.

and a macro lens (AF 90 mm, Tamron) were employed to capture the shapes of the discharges.

The 0.9-GHz CTLR device was employed to observe the influence of the input power or gas flow because it showed the most stable discharge formation among the CTLRs. To determine the effect of the gas flow on discharge formation, an atmospheric pressure chamber was used. Because the discharge formation without gas flow should be examined to identify the effect of the gas flow, a gas-filled environment was required. A transparent acrylic cylinder 50 mm high and 150 mm in diameter was used. It was covered with Teflon top and bottom caps. The acrylic cylinder had four holes for one gas input, two gas outputs, and one insertion hole for CTLR devices. The working gas was supplied through the gas input hole to achieve a high concentration of the working gas in the chamber. The two gas output holes were necessary for maintaining atmospheric pressure in the chamber. The gas flow rate through the gas input hole was 5 slm. This was sufficient to sustain Ar or He plasma stably even though the gas flow from the shorted end of the CTLR was 0 slm. An input power of 15 W was chosen in order to clearly observe the changes in discharge formation for both Ar and He.

The emission spectra were characterized by an optical emission spectrometer (USB2000+, Ocean Optics). The optical probe was located along the longitudinal direction of the open end of the devices. Because the highest emission intensity should be less than the maximum measurable intensity of the USB2000+, the distance between the optical probe and the plasma plumes was adjusted according to the maximum intensity in each case. The minimum distance was 7 mm for the 2.45-GHz He plasma, and the maximum distance was 13 mm for the 1.4-GHz Ar plasma. The integration time was 100 ms, and five scans were averaged. All the emission values were normalized by the highest emission line.

The gas temperature was measured by a thermocoupler (FTI-10, FISO). The probe was located 8 mm and 3 mm away from the end of the CTLRs for Ar and He plasmas, respectively. The probe did not affect the discharge formation and resonance frequency. Unlike low-frequency plasmas, microwave-frequency plasmas are rarely affected by nearby dielectrics or metals. The underlying physics will be studied in the near future.

All the experiments except for the gas flow effect were conducted in ambient air.

## III. RESULTS

### A. Characteristic formation of Ar and He discharges in microwave frequency band

The shape of a discharge is an important feature for biomedical applications. The application method can be varied according to the discharge shape. For example, plasma jets can be used for direct contact treatment, and confined plasmas between electrodes can be applied for afterglow treatment or as a source of light emission. CTLR devices are typically used for direct contact treatment by an Ar plasma plume; however, the discharge shape varied with the gas composition and frequency.

Figure 3 shows side views of the plasma plumes at each frequency. The Ar discharges formed contracted plasma plumes having a stationary filament located axially at the center of the plume, with glowing regions nearby (Figure 3(a)).[23] The Ar plasma plume fluttered as the frequency increased. The 0.9-GHz device showed a stationary Ar plasma plume, and the end of the 1.4-GHz plasma plume fluttered slightly. At 2.45 GHz, the Ar plasma plume moved randomly and fluttered rapidly at the cross section of the inner electrode end. Ar discharges in CTLRs exhibit a unique standing striation pattern. This pattern was observed by the naked eye at the end of the Ar plasma plumes. In the He plasma, a circular glow-like discharge occurred along the edge of the inner electrode instead of forming a plume or a filament (Figure 3(b)). The He plasma converged on the edge of the inner electrode as the frequency increased. As the glowing region of the He plasma became smaller, the bright region constricted and intensified with increasing frequency. When the frequency was 2.45

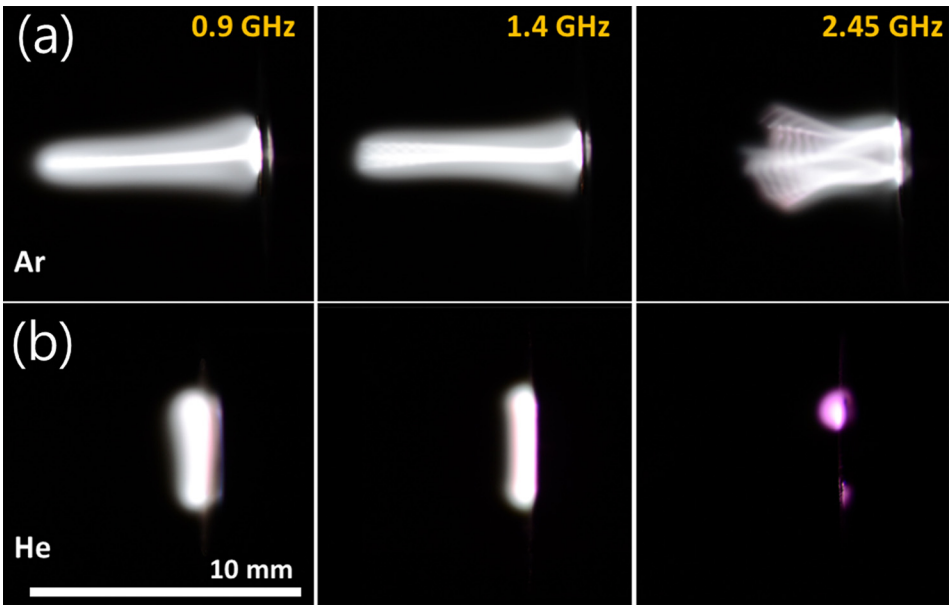


FIG. 3. Side views of microwave (a) Ar and (b) He discharges for frequencies of 0.9, 1.4, and 2.45 GHz.

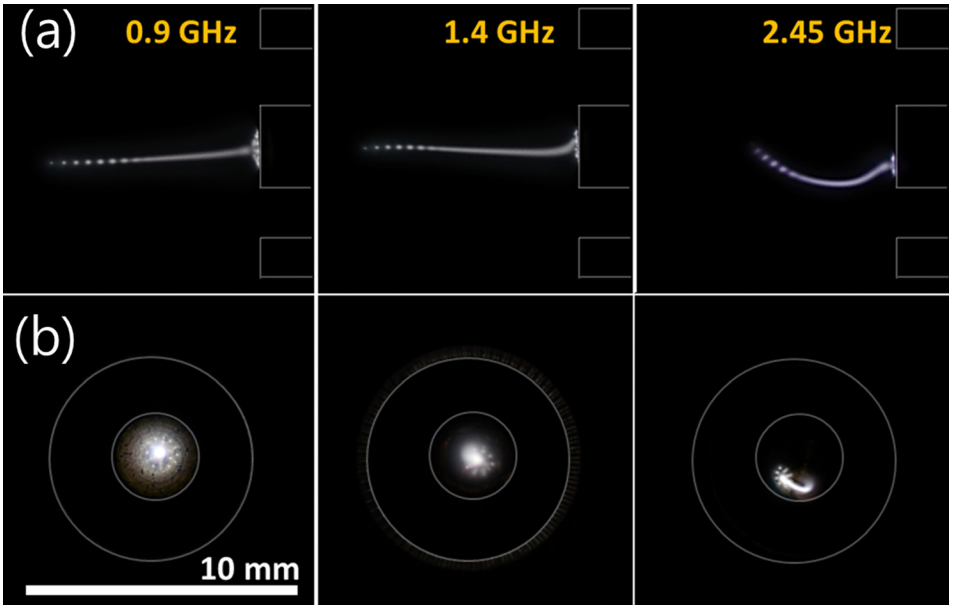


FIG. 4. (a) Side views and (b) front views of Ar discharges for frequencies of 0.9, 1.4, and 2.45 GHz.

GHz, the He plasma was confined at one point. This differs greatly from low-frequency discharges (∼kHz) because He discharges usually generate longer and more stable plumes than Ar discharges in low-frequency plasmas.[4]

The rapid shutter speed (1/8000 s) of the camera enabled clear observation of filaments and an intensified region (Figures 4 and 5). The axial filament and standing striation pattern at the end of the filament were clearly observed in side views of the Ar plasmas (Figure 4(a)). While the 0.9-GHz Ar plasma formed a straight filament, the 1.4-GHz Ar plasma bent slightly, and the 2.45-GHz Ar plasma clearly curved. It is noteworthy that the 2.45-GHz Ar plasma exhibited only one filament, which moved randomly on the cross section of the inner electrode and fluctuated very quickly. The fluctuation might be caused by a combination of the E-field and gas flow forces because a longitudinal force should be required for the motion, which was similar to that of a flag fluttering in the wind. This will be discussed further in Secs. III B and IV A. Increasing contraction was clearly observed in the front views (Figure 4(b)). While the starting area of the Ar plasma plume covered more than one-quarter (∼1.85 $mm^2$) of the cross section (∼7.07 $mm^2$) of the inner electrode in the 0.9-GHz Ar plasma, the starting area (∼0.35 $mm^2$) was approximately 20 times smaller than the cross section of the inner electrode at 2.45 GHz. The radial striation pattern at the starting point was also an interesting feature of the Ar discharge in the CTLR (Figure 4(b)).

Figure 5 shows the constricted glow-like discharge of the He plasmas as the frequency increased. The front view clearly shows the circular discharge along the inner electrode edge. The bright region intensified as the frequency increased from 0.9 GHz to 1.4 GHz. However, the glowing region decreased with increasing frequency. Finally, the He plasma was confined to one point in 2.45-GHz operation. The 2.45-Ghz He plasma stretched toward the outer electrode instead of spreading along the inner electrode (Figure 5(b)). In contrast to the

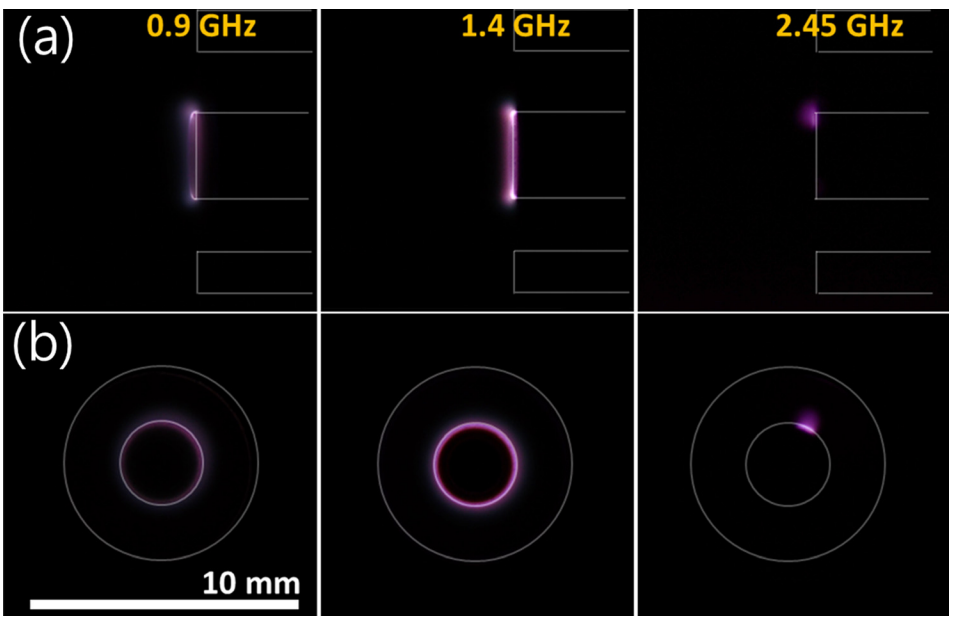


FIG. 5. (a) Side views and (b) front views of He discharges for frequencies of 0.9, 1.4, and 2.45 GHz.

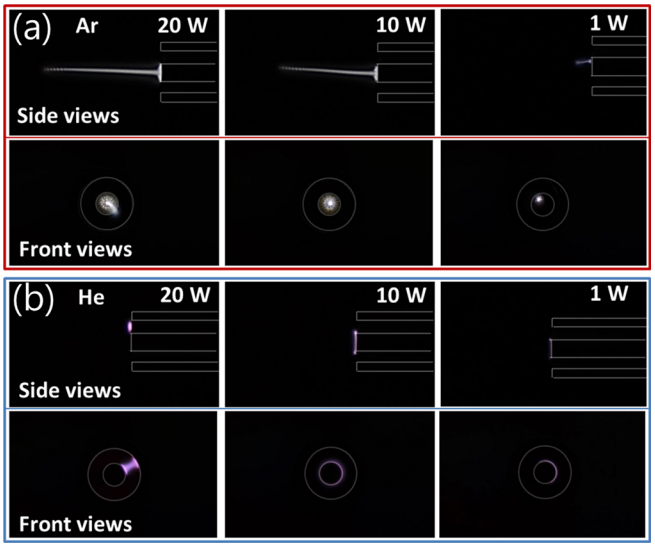


FIG. 6. Side views and front views of microwave (a) Ar and (b) He discharges with different input powers.

Ar discharges, the He discharges were strongly directed toward the outer electrode (ground) rather than being blown out by the gas flow longitudinally as the frequency increased, despite the large gap size. The direction of the He plasma was the same as that of the E-field vectors (Figure 2(b)). The inner electrode leaned slightly to the upper right side (Figure 5(b)) although it was supposed to be located straight along the axial center. As a result, the amplitude of the E-field was the highest at one point, which was where the He discharge was confined at 2.45 GHz. Thus, the He plasmas were influenced significantly by the E-field, and the required power increased in proportion to the operating frequency.

### B. Input power and gas flow effect

It is reasonable that the Ar and He discharges should differ because different gases were used. However, the discharge formation definitely differed from that in low-frequency systems.[4,24,25] Note that the obvious differences were the location and shape of the discharges. The Ar discharge formed a plasma plume and was sustained on the cross section of the inner electrode whereas the He discharge formed a short circular plasma along the edge of the inner electrode. The effect of the E-field and gas flow rate on the shape of the plasma plumes should be observed considering the direction of the plasma plumes.

To examine the effect of the E-field on discharge formation, we varied the input power and fixed the other conditions, including the operating frequency and gas flow rate, because the strength of the E-field is directly related to the input power. The end of the 0.9-GHz Ar plasma plume increasingly fluctuated toward the outer electrode with increasing input power (Figure 6(a)). However, there was no random motion of the filament because the discharge initiation area also increased, covering the entire cross section at 20 W. No significant change was found in the power level from 20 W to the upper limit of the equipment (~40 W). At the low input power, random motion of the filament was observed on the cross section of the inner electrode; however, the filament moved very slowly. The behavior was distinct from that of the 2.45-GHz Ar plasma because the motion was not caused by radial contraction but by a reduction in the volume of the plasma plume due to the low input power. These results indicate that the E-field strength was a dominant factor in the bending or fluctuation of the Ar plasma plume, and the size reduction of the discharge initiation area caused random motion of the Ar plasma plume. In the He plasma (Figure 6(b)), He discharge occurred circularly at a moderate input power level (~10 W) on the edge of the inner electrode. When the input power level was greater than 20 W, the He discharge suddenly formed a path between the inner and outer electrodes. At low input powers (below 1 W), the discharge was ultimately sustained weakly near one point. Because the E-field was insufficient to sustain a circular He plasma at power levels below 1 W, the He plasma could be sustained only near the point of the highest E-field.

The effect of the gas flow should be considered because the gas flow imparted a constant velocity to the particles. The longitudinal force originated in the pressure of the gas flow and was the second strongest force, after the E-field. We structured an atmospheric gas chamber to start the gas flow at 0 slm.

We could identify phases according to the discharge shapes. For the Ar discharge, the discharge shape could be categorized into four phases as the gas flow increased (Figure 7(a)). The Ar plasma formed a path between the inner and outer electrodes in phase 1, and an arched plasma

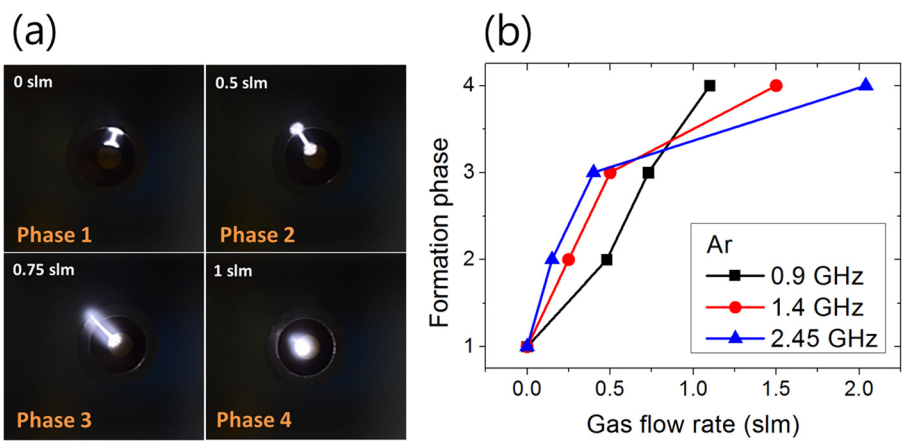


FIG. 7. (a) Front views of microwave 0.9-GHz Ar discharge with different gas flow rates. (b) Change in formation phase versus gas flow rate for 0.9-, 1.4-, and 2.45-GHz discharges.

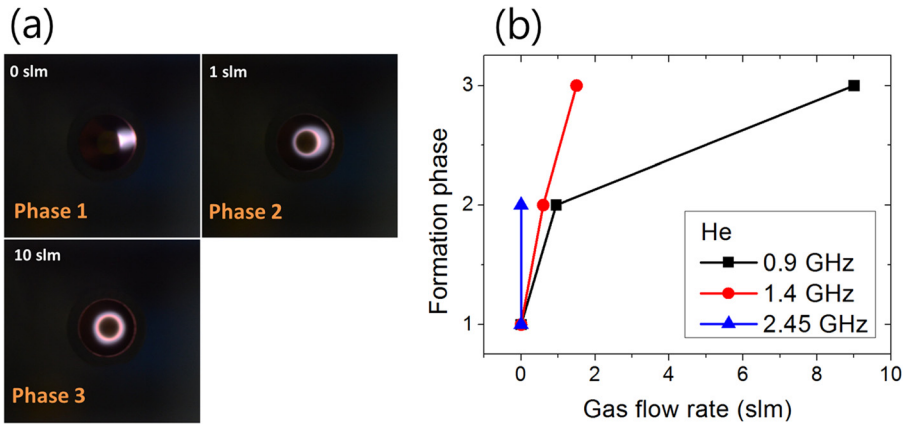


FIG. 8. (a) Front views of microwave 0.9-GHz He discharge with different gas flow rates. (b) Change in formation phase versus gas flow rate for 0.9-, 1.4-, and 2.45-GHz discharges.

path was formed between the electrodes in phase 2. In phase 3, the plasma plume bent toward the outer electrodes, and in phase 4, a straight plasma plume formed in the longitudinal direction. The phase transitions up to phase 3 required a smaller gas flow rate as the frequency increased (Figure 7(b)). This might be the result of contraction. The thickness of the Ar plasma plume decreased with increasing frequency, and the discharge initiation area (phases 1 and 2) on the electrodes was also reduced as the frequency increased. This might make it difficult to sustain the plasma path. On the other hand, phase 4 required a higher gas flow rate as the frequency increased (Figure 7(b)). Considering that phase 4 involves the longitudinal formation of Ar plasma plumes, this result indicates that the E-field was more important than the gas flow in the formation of the longitudinal Ar plasma plume at higher frequency. The 2.45-GHz operation clearly differed from that at the lower frequencies. Although phases 1 and 2 of the 2.45-GHz Ar plasma had shapes similar to those at the lower frequencies, the Ar plasma plume moved rapidly and randomly in phases 3 and 4. The bending of the Ar plasma plume to the outer electrode was reduced as the gas flow rate increased.

Similarly, the He discharge could be categorized into three phases (Figure 8(a)). The He plasma formed a path between the electrodes in phase 1. In phase 2, circular discharge along the edge of the inner electrode was observed, and in phase 3, the He plasma exhibited a strong attraction of the glow region to the outer electrode. In contrast to the Ar discharges, the gas flow rate required for phase transitions was reduced as the frequency increased in the He discharges (Figure 8(b)). The transition between phases 1 and 2 occurred at similar low gas flow rates in both the 0.9- and 1.4-GHz discharges. For phase 3, the gas flow rate required in the 0.9-GHz He plasma was ~5 times higher than that in the 1.4-GHz plasma. Considering mainly the glow region of the He discharges attracted by the E-field, the reduction in the glow region led to faster phase transitions than at lower-frequency operation. The 2.45-GHz He discharge showed distinct features. Its phase remained 2 from a flow rate of 0 slm to the measurement limit of the gas flow meter (10 slm). The discharge region extended to inside of the CTLR, rather than toward the outer electrode, into the shape of the E-field distribution shown in Figure 2(b) (Figure 9). He plasma occurred only on the side with the highest E-field at 2.45 GHz. This is consistent with the explanation that the E-field rapidly became a dominant factor for ionization as the frequency increased.

It is valuable to note that the Ar plasma formed a path between the electrodes without gas flow, similarly to the He discharges. The phase transitions until phase 3 occurred below 1 slm, and the highest gas flow rate was 2 slm for phase 4 in Ar plasmas (Figure 7(b)). This indicates that the gas flow contributed significantly to the formation of the Ar plasma plume, and ambipolar motion could be important for Ar discharges. On the other hand, the He plasmas were rarely influenced by the gas flow rate. They required a much higher gas flow rate for phase transitions than the Ar plasmas (Figure 8(b)), and the shape of the intensified region did not change with the gas flow rate except in phase 1.

### C. Breakdown and sustain powers

The breakdown and sustain powers are also important parameters for biomedical applications because they can determine the system size and electrical safety. Figure 10 shows the breakdown and sustain powers of the Ar and He plasmas. The breakdown power of the Ar plasma decreased as the frequency increased; its sustain power decreased slightly at 1.4 GHz and increased again at 2.45 GHz. The breakdown and sustain powers of the He plasma decreased at 1.4 GHz and then increased at 2.45 GHz. Finally, the breakdown power of the He

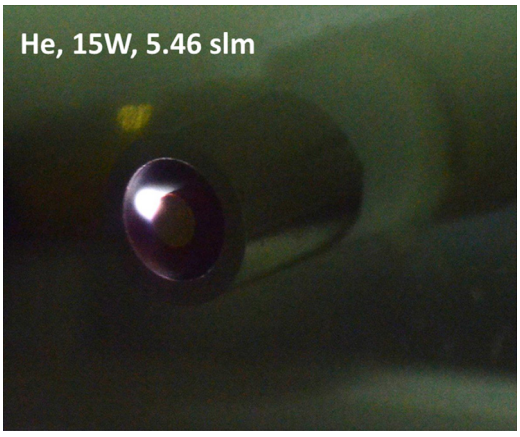


FIG. 9. Distinct discharge formation in 2.45-GHz He plasma. The formation was similar to the E-field distribution.

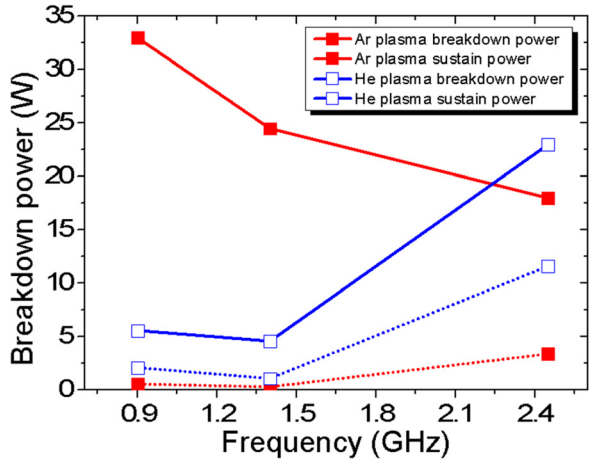


FIG. 10. Breakdown powers (solid lines) and minimum sustain powers (dotted lines) of Ar (red solid squares) and He (blue open squares) plasmas.

plasma became higher than that of the Ar plasma for 2.45-GHz operation. The results showed a distinctive trend unlike that for low-frequency discharges. Although both the breakdown and sustain powers of the Ar plasma were higher than that of the He plasma at low frequency, the sustain power of the Ar plasma was lower than that of the He plasma at the microwave frequency.[2,24] The difference between the breakdown and sustain powers of the Ar plasma was almost 30 W at 0.9 GHz and decreased as the frequency increased. However, the difference between the breakdown and sustain powers of the He plasma was clearly smaller than that of the Ar plasma (~3 W).

### D. Optical emission spectra

Ultraviolet–visible emission spectra of the plasmas showed various species generated in them (Figure 11). Ar and $N_2$ species were observed in the Ar discharges (Figure 11(a)), and the Ar 763.5-nm peak was the highest peak. The reactive oxygen species atomic O (777.4 nm) and hydroxyl radicals (·OH) (309 nm) were also observed. The $N_2$ second positive band, NO–$\gamma$ band, and Ar subpeaks obviously increased with increasing frequency. The $N_2$ 337-nm line in particular was increased within the $N_2$ second positive band.

In the He plasmas, the ·OH peak (309 nm) was the highest peak at 2.45 GHz but not at the lower frequencies (Figure 11(b)).[4,26] The $N_2$ second positive band and NO–$\gamma$ band also increased with increasing frequency whereas the He peaks were reduced. The intensity of the $N_2$ 337-nm line was greatest at 2.45 GHz.

### E. Estimation of plasma impedance, electron density, and efficiency

The input impedance of the CTLRs was influenced by the plasma impedance because the load impedance at the open end changed when the plasma ignited. Thus, the plasma impedance affects the performance and efficiency of microwave devices. The plasma impedance can be estimated by fitting the calculated reflection coefficient ($S_{11}$) to the measured value. A detailed procedure based on transmission line theory is described in the literature.[3,19,22] Figure 12 compares the calculated and measured $S_{11}$. The measured data (open circles) agreed well with the calculated data (solid lines) at certain plasma impedances. The impedance of the Ar plasma was 860-j160, 831-j596, and 790-j710 Ω at 0.9, 1.4, and 2.45 GHz, respectively (Table I). The real part of the impedance decreased, and the imaginary part increased as the frequency increased. The impedance of the He plasma was 3550-j1530, 2990-j2357, and 2815-j3100 Ω at 0.9, 1.4, and 2.45 GHz, respectively (Table I). The impedances of the He plasma were four times those of the Ar plasma.

The electron density ($n_e$) can be estimated using the following equation:[3,19,22,27]

$$n_e = \frac{L_{bulk} m_e \upsilon}{R_p q^2 A_{bulk}}. \quad (1)$$

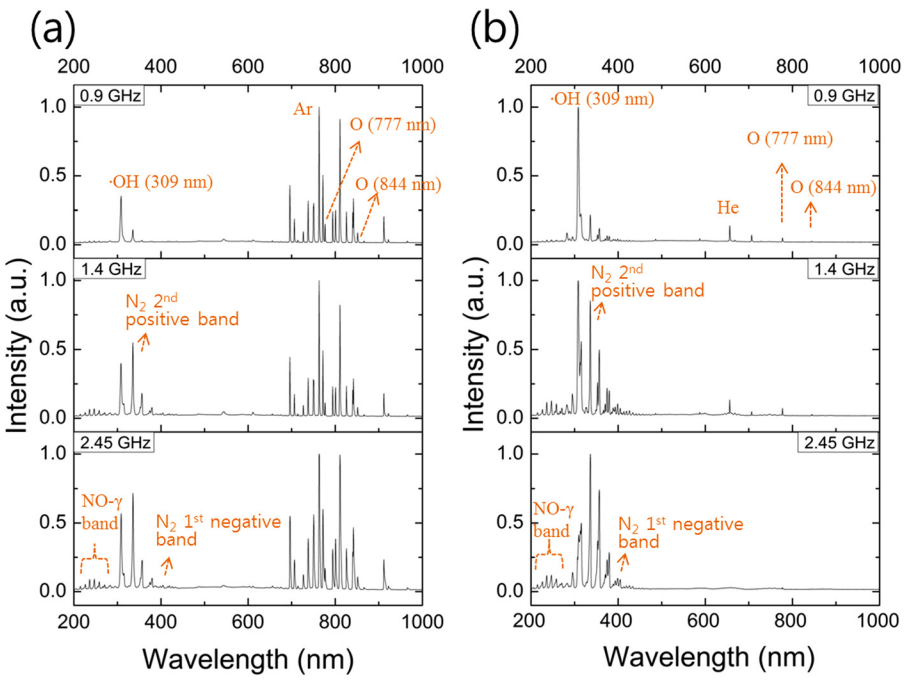


FIG. 11. UV–visible emission spectra of microwave (a) Ar and (b) He plasmas.

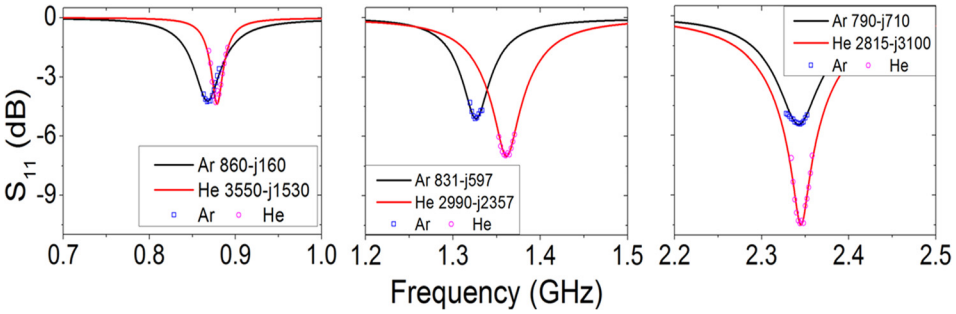


FIG. 12. (a) Comparison of measured and calculated $S_{11}$ with the plasma impedances.

$L_{bulk}$ and $A_{bulk}$ are the length and area of the discharge, respectively. The discharge geometry was assumed to be cylindrical for Ar plasmas and ring-shaped for He plasmas. Further, $m_e$ is the electron mass and $\upsilon$ is the electron collision frequency. The electron collision frequencies were $5.49451 \times 10^{12}$ and $6.28931 \times 10^{12}$ for Ar and He, respectively, at 310 K and atmospheric pressure.[28] $R_p$ is the real part of the plasma impedance. The electron density increased as the frequency increased (Table I), and the Ar plasmas showed approximately 2.5 log-order larger electron densities than the He plasmas. The higher electron densities in Ar plasmas are consistent with previous studies.[29,30]

The efficiency of the CTLRs could be estimated by transmission line theory. The power transferred by the plasma can be expressed as the sum of the incident waves to the open end including reflected waves from the shorted end. The detailed procedure is described in the literature.[3,19] As shown in Eq. (8) in Ref. 3, the reflection coefficient $[\Gamma = (Z_P - Z_0)/(Z_P + Z_0)]$ and the quality factor $[Q = f_C/(f_2 - f_1)]$ are important components of the efficiency. $Z_P$ is the plasma impedance, and $Z_0$ is the characteristic impedance of the CTLRs. The frequency variables, $f_C$, $f_1$, and $f_2$, are the central resonance frequency, lower −3 dB frequency, and upper −3 dB frequency, respectively. They were chosen from the measured $S_{11}$ profiles (Figure 12). The efficiencies of the CTLRs are presented in Table I for each working gas. Ar plasmas were more efficient than He plasmas, and the efficiencies decreased as the frequency increased.

### F. Gas temperature

The gas temperature is an important consideration for biomedical applications. Because the plasmas generally contact or are located near the target for treatment, there should be no thermal damage. Figure 13 shows the measured gas temperatures of the Ar and He plasmas. In contrast to the case for low-frequency systems, the He plasmas showed higher gas temperatures than the Ar plasmas. The gas temperatures of the Ar plasmas were 47.9, 50.4, and 39.2 °C at 0.9, 1.4, and 2.45 GHz, respectively, and those of the He plasmas were 67.3, 69.1, and 66.5 °C at 0.9, 1.4, and 2.45 GHz, respectively. The temperatures of both the Ar and He plasmas were lowest at 2.45 GHz. This might be caused by the abnormal plasma formation at 2.45 GHz in both Ar and He.

TABLE I. Estimated plasma impedance, electron density, and efficiency of CTLRs for each frequency.

| | Plasma impedance (Ω) | | Electron density ($cm^{-3}$) | | Efficiency (%) | |
|---|---|---|---|---|---|---|
| Frequency (GHz) | Ar | He | Ar | He | Ar | He |
| 0.9 | 860-j160 | 3550-j1530 | $9.53 \times 10^{14}$ | $3.81 \times 10^{12}$ | 71.15 | 52.54 |
| 1.4 | 831-j596 | 2990-j2357 | $1.80 \times 10^{15}$ | $5.33 \times 10^{12}$ | 65.61 | 25.92 |
| 2.45 | 790-j710 | 2815-j3100 | $4.16 \times 10^{15}$ | $6.74 \times 10^{12}$ | 64.61 | 21.19 |

## IV. DISCUSSIONS

### A. Distinctive formation of Ar and He discharges in microwave frequency band

Microwave Ar plasmas showed distinct formation from low frequency plasmas such as radial contraction, random motion, fluttering, and radial striation pattern. Radial contraction in microwave Ar plasmas is known to be mainly related to radially non-uniform heating.[7] Previous researchers suggested low thermal conductivity, high electron density, and the skin effect of a high-frequency E-field as factors in the radial non-uniformity, and these factors led to contraction.[7] Their suggestions are consistent with our experimental results because Ar has a relatively low thermal conductivity ($17.72 \times 10^{-3}$ $W \cdot m^{-1} \cdot K^{-1}$), a microwave Ar plasma generates abundant electrons, and the skin effect is considerable at microwave frequencies.[3,20] Moreover, as the frequency increased, the bulk region increased, and the power dissipated in the bulk region also increased (α mode). This led to less efficient ionization and a reduction in the plasma volume as the frequency increased, owing to frequent elastic

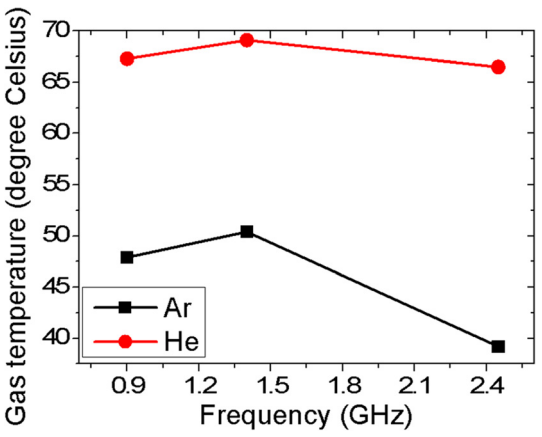


FIG. 13. Measured gas temperatures at the end of the plasma plumes for different frequencies for Ar (black squares) and He (red circles).

collisions in the bulk.[20] These reasons could explain the increasing contraction of the microwave Ar plasma with increasing frequency. The detail will be discussed in the He discharge cases.

Random motion and fluttering of the plasma plume in the 2.45-GHz Ar plasma were reported in several microwave Ar discharge systems, including surface-wave-sustained plasmas.[6,32,33] The phenomenon, called filamentation, is known to be related to the radial non-uniformity of the microwave E-field. Kabouzi *et al*. showed that the frequency was an effective factor in filamentation.[7] In addition, filamentation might be closely related to contraction phenomenon. As the size of the discharge initiation area decreased with increasing frequency, the E-field distribution became more uniform. Plasma has a finite conductivity. Thus, the area in contact with the plasma had a weaker E-field than the surroundings. As the discharge area increased, the E-field distribution on the cross section of the inner electrode exhibited increasing interference. The cross section of the inner electrode could maintain the E-field strength when the discharge initiation area was small. Thus, the Ar discharge could be sustained at all the points of the cross section of the inner electrode end, and the filament could move randomly.

The radial striation pattern was attributed to the motion of plasma bullets. The departure of plasma bullets had been observed around the axial center using an intensified charge-coupled device technique.[34] The bullets were generated around the axis and merged alternately to the center filament. The striation pattern and alternating motion may be caused by the circular E-field distribution and dipole–dipole repulsion.[35,36] The cross section of the inner electrode had a circular E-field distribution (Figure 2(a)), and there were vectors toward the axial direction (Figure 2(b)). Plasma bullets were generated and moved following this direction. Although the cross section of the inner electrode had the second strongest E-field, there was a high possibility that Ar plasma could be sustained on the cross section owing to the low ionization level (15.8 eV) and metastable levels (11.5 and 11.7 eV) of Ar.[6,11] Moreover, neutral atoms in the Ar metastable state excited by electrons between the electrode gap could be blown in the longitudinal direction by the gas flow and contributed to sustaining the Ar plasma plume.

In contrast to the low-frequency behavior, He plasma formed a confined plume at microwave frequencies, and showed bright intensified region closer to electrode.[7,37,38] The phenomenon agrees with the result for a capacitively coupled plasma (CCP) in the RF band in Ref. 37. The study observed reduction of sheath region with increasing frequency. Power coupled to electrons was increased, and electron loss by escaping to the electrodes was reduced also because of rapid change of sinusoidal RF E-field.[31] This led to the constriction of the emitting layer near electrodes.

The results of He discharge formation in 0.9 and 1.4 GHz consistent with the trend in previous researches in Ref. 37; however, 2.45-GHz He plasma showed extreme volume reduction and weakened. This result might be caused from high ionization and excitation energy of He and change of dominant ionization process with increasing frequency. McKay *et al*. reported the reduction in electron density after mode transition.[20] When the operating frequency is over a criterion, mode transition ($\gamma$–$\alpha$) is occurred. Before the mode transition, electron density increases rapidly with increasing frequency as mentioned in the explanation of constriction phenomenon. After that, the electron density decreases gradually as frequency increases. It was caused by the reduction of sheath region leading to the reduction of secondary electrons and Penning ionization. The influence of the sheath reduction might exceed that of increasing power coupled to electrons and reducing electron loss. He has a higher ionization energy (25.4 eV) than other noble gases such as Ar (15.8 eV) and $N_2$ (15.6 eV for $X^2\Sigma_b^+$ and 18.7 eV for $B^2\Sigma_u^+$), and the energy level of He metastable atoms (19.8 and 20.6 eV) is higher than the ionization level of $N_2$.[6,11] Thus, Penning ionization of He and $N_2$, and that between them, was the main mechanism for sustaining He discharge in low-frequency systems.[11–14] As the frequency increased, the sheath size was reduced, and the power dissipation in the bulk increased ($\alpha$ mode). This reduced the effective excitation and ionization such as Penning ionization by background $N_2$ because ionization through background gas are most active in the sheath regions.[20,37] Consequently, direct impact and stepwise ionization of He became important electron generation processes in high-frequency systems.[9,37] This means that higher-energy electrons were needed with increasing frequency, and a stronger E-field was required to sustain the plasma as a result. Accordingly, the 2.45-GHz He discharge was induced at one side of the inner electrode where the amplitude of the E-field was the highest.

In low frequency He plasmas, plasma plume is known to be the propagation of plasma bullets. Many researchers showed simulated and experimental results to explain the phenomena.[11–16] Continual ionization at the bullet head enable the propagation of bullets. In the mechanism of continual ionization, Penning ionization has been regarded as a dominant ionization process in He plasma.[11–14] On the other hand, Naidis *et al*. showed simulated results of dominant role of He metastable species, ions, and direct impact ionization in DC nanopulsed He plasma.[15,16] Although the issue needs further study, it is true that Penning ionization plays important role in low frequency He plasmas. Based on our previous study, high energy electrons for ionize He by direct impact ionization were very few in the condition.[4] Adding this, when we reduced air contents at the open end of the CTLR, the breakdown power was increased. We covered a 15-cm long tube at the open end of CTLR. He gas met ambient air at the end of tube, and there was almost pure He gas at the open end of CTLR. In this experiment, the breakdown powers were increased ~1.6, ~1.5, and ~1.2 times in 0.9, 1.4, and 2.45 GHz, respectively. This indicates the important role of $N_2$ and Penning ionization, and reduction of the Penning ionization process as frequency increased. Considering above, the difference of He plasma formation in low frequency and microwave frequency could be explained by the sheath reduction and following reduction of Penning ionization process with increasing frequency in this study.

Interestingly, discharge formation at 1.4 GHz and 2.45 GHz differed significantly for both the Ar and He discharges. This might indicate an optimal boundary of the

microwave frequency band under the experimental conditions, considering that Kwon *et al*. presented an optimal frequency by a particle-in-cell simulation in the microwave frequency band.[8]

Input power and gas flow effects gave insights for the distinct discharge formation in microwave bands. It is reasonable that the effect of the E-field on plasmas is proportional to the input power level because the input power is directly related to the E-field at the open end of the CTLRs. Bent and fluctuating Ar plasma plumes were observed at power levels above 20 W. Considering that they were more common as the frequency increased, this result means that the effect of the E-field increased as the frequency increased. At low powers (below 1 W), random motion was observed similar to that in the 2.45-GHz Ar plasma. This can be explained by the volume reduction of the Ar plasma plume. As mentioned above, the E-field distribution on the cross section of the inner electrode was less affected as the discharge initiation area became smaller. For the He plasma, the result can be explained in the same manner. A strong attraction of the He plasma toward the outer electrode was observed at high power levels, similar to that in the 2.45-GHz He plasma. At low power levels, a reduction in the volume and confinement to one side of the inner electrode were also observed.

The power coupled to electrons in the bulk increased in proportion to the operating frequency,[8,39] and the abundant heated electrons moved along the direction of the E-field ignoring other forces, including the gas flow pressure, owing to the low mass of electrons. Thus, there was a high possibility of generating ions and excited species along the direction of the E-field. This can explain the increasing E-field influence as the frequency increased. The similarity between the behavior at low power and in some of the 2.45-GHz plasmas can be explained by a mode transition with increasing frequency. While the volume reduction was the result of insignificant energy for ionization and excitation at low powers, contraction or constriction caused the volume reduction at microwave frequencies.[37] The electron generation process changed from $\gamma$ mode to $\alpha$ mode as the frequency increased, and the required energy became higher, as mentioned above.[6,9,11,20,37] He plasmas were influenced more significantly than Ar plasmas because of their high ionization and excitation energies.

The gas effect experiments suggested different types of discharge formation in Ar and He. The Ar plasma was influenced more strongly by gas flow than the He plasma at microwave frequencies. The different characteristics and dominant ionization processes of the working gases could be the main reasons. Owing to the relatively high mass of Ar, ions and excited species of Ar generated between the inner and outer electrodes could be forced out longitudinally by the gas flow.[40] Some of the ions and excited species would be lost diagonally outward, and some of the species would move in a longitudinal direction or diagonally inward during repeated excitation and de-excitation through interactions with other particles. The motion of Ar ions induced ambipolar motion, and excited species contributed to the ionization. On the other hand, Ar ions and excited species could be generated on the cross section of the inner electrode, considering the low ionization and excitation energies of Ar. Thus, there was a high possibility that abundant ions and excited species were gathered in the front of the cross section of the inner electrode. Ar ions are known to have important roles in forming plasma jets according to Dawson's theory.[14] The direction of the E-field is another factor in Ar plasma plume formation. When the Ar plasma plume is generated, the E-field direction should change to a longitudinal direction through the plume because the plasma bulk has a finite conductivity. Consequently, excited Ar species and Ar ions felt a longitudinal force from both the E-field and the gas flow. This might lead to ionization and longitudinal motion of the bullets and, as a result, Ar plasma jet formation.

In the He discharges, it was clear that the He plasma was rarely affected by the gas flow, and the He discharges required a stronger E-field for sustenance than the Ar discharges in the microwave frequency band. These results coincide with the above explanation. In the low-frequency discharges, electron generation occurred mostly in the sheath region ($\gamma$ mode). Secondary electrons and Penning ionization cause electron avalanches inside the sheath region.[41] As the frequency increased, the power coupled to electrons increased, and electron generation occurred outside the sheath regions; the electrons in the bulk were the dominant contributors to sustaining the discharge ($\alpha$ mode).[8,20] Thus, much of the energy was transferred through elastic collisions in the bulk region rather than inelastic collision in the sheath regions, and ionization and excitation processes through the background gas become less frequent.[20,41] As a result, the Penning ionization rate between He and $N_2$ decreased, and the He discharge required a higher E-field than at low frequency. Thus, He discharges could be sustained only at the edge of the inner electrode; furthermore, the 2.45-GHz He plasma was generated only at one side of the inner electrode edge. Another important factor arises from the light mass, high diffusion constant to air, and high thermal conductivity of He. These caused a high loss rate of He ions and excited species to air. There is also a lack of He ions and excited species on the front of the inner electrode due to the high ionization and excitation energies. Consequently, He discharges could form only a confined plasma.

### B. Frequency effect on electrical properties and suitability for biomedical applications

The results of breakdown and sustain powers might be governed by the same underlying physics as the plasma formation results related to the change in the dominant ionization process as the frequency increased. In the Ar discharges, stepwise ionization and direct impact ionization of Ar could be the main electron generation processes, not only Penning ionization between Ar metastable species and through $N_2$ metastable species, owing to the low excitation (11.5 and 11.7 eV) and ionization (15.8 eV) energies of Ar.[6,11] Thus, the Ar discharges have advantages over He discharges in sustaining the discharge at microwave frequencies. The mode transition ($\gamma$–$\alpha$) and reduction in the sheath regions with increasing frequency increase had a negative effect on the He discharges owing to the high ionization (25.4 eV) and

excitation (19.8 and 20.6 eV) energies of He.[11,26] The required energy became higher as the frequency increased because the Penning ionization through $N_2$ in the sheath regions was reduced.[20,37] This could reverse the breakdown powers of Ar and He at 2.45-GHz operation. In terms of the power coupled to electrons, the breakdown or sustain power should decrease as the frequency increases. However, interestingly, the breakdown and sustain powers of He and the sustain power of Ar increased at 2.45 GHz, where they were the highest for each plasma. This might be caused by the change in the dominant ionization processes, as we mentioned above. The influence of the change in the dominant ionization processes exceeded the influence of the increase in the power coupled to electrons between 1.4 and 2.45 GHz. Thus, 1.4 GHz might be the tradeoff point for the two effects.

Optical emission spectra showed various components and the change of the components with increasing frequency. An increase in the $N_2$ second positive band and NO–$\gamma$ band were common phenomenon in both the Ar and He discharges. The $N_2$ second positive band required more than 11.1 eV; other paths for excitation of $N_2$ could start from metastable state He and Ar, and they also required higher energy.[11,42–44] The NO–$\gamma$ band was induced by $N_2$ ($A^3\Sigma_u^+$), mainly by the following reactions:[45,46]

$$N_2\left(A^3\Sigma_u^+\right) + NO\left(X^2\Pi\right) \rightarrow N2\left(X^1\Sigma_g^+\right) + NO\left(A^2\Sigma^+\right), \quad (2)$$

$$NO\left(A^2\Sigma^+\right) \rightarrow NO\left(X^2\Pi\right) + h\nu(\text{NO-}\gamma\text{ band}). \quad (3)$$

The $N_2$ ($A^3\Sigma_u^+$) state required at least 6.17 eV.[46,47] This result is consistent with the previous finding that the number of high-energy electrons increased as the frequency increased.[2,8,20,39] Furthermore, the increase in the electron density and the volume reduction lead to increased collisions between particles, and this leads to the generation of abundant NO-$\gamma$ and $N_2$ species as the frequency increases.

For biomedical applications, reactive species such as ·OH, atomic O, and NO were important contributors. ·OH and O have been known as key components in sterilization and tooth whitening,[26,48,49] and NO has been known to contribute significantly to wound healing and blood coagulation.[5,50] The portion of reactive species changed as the frequency changed (Figure 14). In the Ar plasmas (Figure 14(a)), the intensity of ·OH and NO emissions were proportional to the frequency. ·OH and NO emissions increased approximately two-fold overall from 0.9 to 2.45 GHz. On the other hand, the intensity of atomic O (777 and 844 nm) decreased at 1.4 GHz and increased again at 2.45 GHz. It is possible that the operating frequency can be chosen on the basis of these results. For example, the 2.45-GHz Ar plasma is appropriate for wound healing and sterilization owing to the higher ·OH and NO densities than at lower frequencies. In the He plasmas (Figure 14(b)), the ·OH intensity was maximum at 0.9 and 1.4 GHz and reduced at 2.45 GHz. The intensity of atomic O (777 nm) showed a similar trend. The NO emission increased at 1.4 GHz, but there was little difference between 1.4 and 2.45 GHz. The 1.4-GHz He plasma showed the best performance among the He plasmas. It can be applied for sterilization or tooth whitening, considering that the ·OH and O (777 nm) peaks were the highest. The reduction in the ·OH and O peaks at 2.45 GHz might be caused by the instability of the 2.45-GHz He plasma, including extreme constriction. The reduction of He peaks and increase of $N_2$-related peaks in He plasmas might be related to the less efficient ionization with increasing frequency.

Impedance, electron density, and power efficiency of the plasmas estimated from the influence of the plasmas to $S_{11}$ of CTLR. Because He plasmas have a higher impedance than Ar plasmas, they have less effect on the performance of CTLRs. The volume and location of He plasmas could be one of the reasons, considering that the microwave signal transmission is significantly influenced by the length of the conductor. The volume of the He plasmas was small, and the location was limited to near the edge of the inner electrode, in contrast to Ar plasma generation as an extension of the inner electrode.

The electron density is related to the excitation and ionization energies of the working gases. Because Ar has lower excitation and ionization energies than He, abundant electrons could be generated in the Ar plasmas. It is noteworthy that the estimated electron density increased with increasing frequency; however, breakdown or sustenance became difficult at 2.45 GHz. This might be caused by the reduction of the plasma volume because the density is inversely proportional to the volume.

The trend in power efficiency is related to the reduction in efficient ionization such as Penning ionization as the frequency increases.[20,41] Owing to the high ionization and excitation

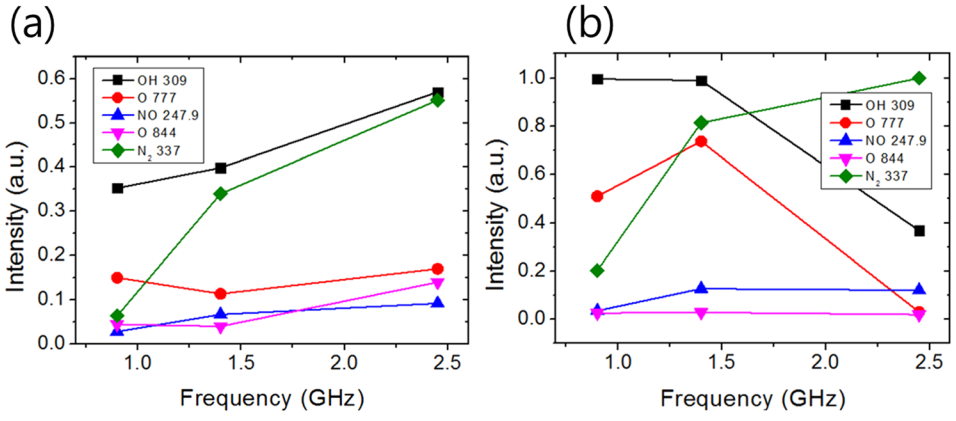


FIG. 14. Change in intensity of reactive species ·OH, O, NO, and O, and $N_2$ band for (a) Ar and (b) He plasmas at different frequencies.

energies of He, the efficiency decrease was more significant for the He plasma than for the Ar plasma. The result differs from the earlier result in Ref. 3, which showed that a He plasma was more efficient than an Ar plasma. This is reasonable because the CTLR in that study had a tip to reduce the gap size and breakdown power. With the small gap (40 $\mu$m), the formation shape of the plasma was totally different.

The higher gas temperatures of He plasmas than Ar plasmas might be caused by the higher sustain power of He plasmas. This could be explained by the change in the dominant ionization processes with increasing frequency, as mentioned above. The occurrence of the lowest temperature at 2.45 GHz in both Ar and He might be related to the noticeable change in discharge formation at 2.45 GHz. The Ar plasmas showed rapid random plume motion on the cross section of the inner electrode, and the He plasmas were extremely confined to one point of the inner electrode edge. Owing to the rapid random motion of the Ar plasmas, sufficient heat could not be transferred to the thermometer probe. This property enabled the 2.45-GHz Ar plasma to generate intensive plasma without thermal damage. He plasmas would be appropriate for afterglow treatment.

In our previous works, the gas temperature of the Ar plasma using 0.9 GHz device was in the range from room temperature (26 °C) to ~45 °C.[4,5,51,52] There were no thermal damages on the living targets such as a skin tissue, bacteria, and a blood drop. Because the gas temperature strongly depends on input power and we fixed high enough power for observation of the characteristics in this study, the gas temperature of microwave Ar plasmas can have easily acceptable gas temperature.

## V. CONCLUSION

We demonstrated the distinctive formation of Ar and He plasmas in the microwave frequency band. We also discussed the characteristics of the plasmas in terms of biomedical applications. The phenomena were obviously different from those of low-frequency (~kHz) plasmas. Ar formed a stable plasma plume, and He formed a short, circular glow plasma along the electrode. As the frequency increased, the Ar plasma plume exhibited contraction and filamentation, and constriction of the He plasma to the electrode was observed. Experiments on the effects of the power and gas flow revealed that the influence of the E-field became dominant as the frequency increased, and gas flow was dominant only for the Ar plasmas. We suggested mechanisms for the distinctive formation of microwave Ar and He plasmas. As the frequency increased, the dominant ionization processes changed, and direct impact ionization became more frequent than Penning ionization through a background gas such as $N_2$.[6,8–11,20,37] This change made it hard to sustain He plasma because He has relatively high ionization and excitation energies. Consequently, He plasma could be sustained only at the highest E-field point and was confined to the edge of the inner electrode.

We measured and estimated the UV–visible emission spectra and electrical properties, including the plasma impedance. The emission spectra indicated an increase in high-energy electrons. The ·OH peak was proportional to the frequency in the Ar plasmas; on the other hand, in the He plasmas, it decreased rapidly at 2.45 GHz. The O peak was maximum at a frequency of 2.45 and 1.4 GHz for the Ar and He plasmas, respectively. For biomedical applications, the operating frequency and working gas could be chosen according to the type of reactive species, ·OH, O, and NO, depending on the applications. The estimated electron density and efficiency showed a clear trend with the frequency. The electron density increased as the frequency increased, and Ar had a higher electron density than He. The efficiency decreased as the frequency increased, and Ar plasmas showed higher efficiency than He plasmas. All the results could be explained in the same manner as the plasma plume formation.

The microwave-excited Ar plasmas generally showed superior properties; however, He plasmas can be employed as well for low-dose treatment. Our study of the characteristics of microwave-excited plasmas can provide helpful information for choosing which frequency and gas will be used in each biomedical application field.

## ACKNOWLEDGMENTS

This work was supported by a National Research Foundation of Korea Grant (NRF-2012-0005437), a grant from the Traditional Korean Medicine R&D project, Ministry of Health & Welfare, Republic of Korea (B110039), and the Brain Korea Plus program, funded by the Korean Government (Ministry of Education, Science and Technology).

[1]M. Moisan, C. M. Ferreira, Y. Hajlaoui, D. Henry, J. Hubert, R. Pantel, A. Ricard, and Z. Zakrzewski, Rev. Phys. Appl. **17**, 707 (1982).
[2]F. Iza, G. J. Kim, S. M. Lee, J. K. Lee, J. L. Walsh, Y. T. Zhang, and M. G. Kong, Plasma Processes Polym. **5**, 322 (2008).
[3]J. Choi, F. Iza, H. J. Do, J. K. Lee, and M. H. Cho, Plasma Sources Sci. Technol. **18**, 025029 (2009).
[4]Y. S. Seo, H. Wk. Lee, H. C. Kwon, J. Choi, S. M. Lee, K. C. Woo, K. T. Kim, and J. K. Lee, Thin Solid Films **519**, 7071 (2011).
[5]J. Choi, A.-A. H. Mohamed, S. K. Kang, K. C. Woo, K. T. Kim, and J. K. Lee, Plasma Processes Polym. **7**, 258 (2010).
[6]E. Castanos-Martinez, M. Moisan, and Y. Kabouzi, J. Phys. D: Appl. Phys. **42**, 012003 (2009).
[7]Y. Kabouzi, M. D. Calzada, M. Moisan, K. C. Tran, and C. Trassy, J. Appl. Phys. **91**, 1008 (2002).
[8]H. C. Kwon, I. H. Won, and J. K. Lee, Appl. Phys. Lett. **100**, 183702 (2012).
[9]J. J. Shi, D. W. Liu, and M. G. Kong, Appl. Phys. Lett. **89**, 081502 (2006).
[10]J. J. Shi and M. G. Kong, Appl. Phys. Lett. **90**, 101502 (2007).
[11]Q. Li, X. M. Zhu, J. T. Li, and Y. K. Pu, J. Appl. Phys. **107**, 043304 (2010).
[12]Q. Li, Y. K. Pu, M. A. Lieberman, and D. J. Economou, Phys. Rev. E **83**, 046405 (2011).
[13]Y. Skiyama and D. B. Graves, Plasma Sources Sci. Technol. **18**, 025022 (2009).
[14]J. L. Walsh, F. Iza, N. B. Janson, V. J. Law, and M. G. Kong J. Phys. D: Appl. Phys. **43**, 075201 (2010).
[15]D. Breden, K. Miki, and L. L. Raja, Appl. Phys. Lett. **99**, 111501 (2011).
[16]Y. Sakiyama, N. Knake, D. Schröder, J. Winter, V. Schulz-von der Gathen, and D. B. Graves, Appl. Phys. Lett. **97**, 151501 (2010).
[17]M. Yousfi, O. Eichwald, N. Merbani, and N. Jomaa, Plasma Sources Sci. Technol. **21**, 045003 (2012).
[18]B. L. Sands, S. K. Huang, J. W. Speltz, M. A. Niekamp, and B. N. Ganguly, J. Appl. Phys. **113**, 153303 (2013).
[19]F. Iza and J. Hopwood, Plasma Sources Sci. Technol. **14**, 397 (2005).
[20]K. McKay, F. Iza, and M. G. Kong, Eur. Phys. J. D **60**, 497 (2010).

[21]S. M. Lee, Y. J. Hong, Y. S. Seo, F. Iza, G. C. Kim, and J. K. Lee, Comput. Phys. Commun. **180**, 636 (2009).
[22]S. K. Kang, Y. S. Seo, H. Wk. Lee, A. Rehman, G. C. Kim, and J. K. Lee, J. Phys. D: Appl. Phys. **44**, 435201 (2011).
[23]E. Castanos-Martinez, Y. Kabouzi, K. Makasheva, and M. Moisan, Phys. Rev. E **70**, 066405 (2004).
[24]Y. S. Seo, A.-A. H. Mohamed, K. C. Woo, H. W. Lee, J. K. Lee, and K. T. Kim, IEEE Trans. Plasma Sci. **38**, 2954 (2010).
[25]X. P. Lu, Z. H. Jiang, Q. Xiong, Z. Y. Tang, and Y. Pan, Appl. Phys. Lett. **92**, 151504 (2008).
[26]H. W. Lee, S. H. Nam, A.-A. H. Mohamed, G. C. Kim, and J. K. Lee, Plasma Processes Polym. **7**, 274 (2010).
[27]M. A. Liebermann and A. J. Lichtenberg, *Principles of Plasma Discharges and Material Processing*, 2nd ed. (Wiley, New York, 2005), p. 80.
[28]D. R. Lide, *2001-2002 Handbook of Chemistry and Physics*, 82nd ed. (CRC Press, 2001).
[29]J. Jonkers, M. van de Sande, A. Sola, A. Gamero, and J. van der Mullen, Plasma Sources Sci. Technol. **12**, 30 (2003).
[30]S.-Z. Li, J.-P. Lim, J. G. Kang, and H. S. Uhm, Phys. Plasmas **13**, 093503 (2006).
[31]S. Hofmann, A. F. H. van Gessel, T. Verreycken, and P. Bruggeman, Plasma Sources Sci. Technol. **20**, 065010 (2011).
[32]Z. Chen, G. Xia, Q. Zhou, Y. Hu, X. Zheng, Z. Zheng, L. Hong, Y. Huang, and M. Liu, Rev. Sci. Instrum. **83**, 084701 (2012).
[33]H. Schluter and A. Shivarova, Phys. Rep. **443**, 121 (2007).
[34]S. K. Kang, A.-A. H. Mohamed, H. W. Lee, and J. K. Lee, IEEE Trans. Plasma Sci. **39**, 2318 (2011).
[35]W. Breazeal, K. M. Flynn, and E. G. Gwinn, Phys. Rev. E **52**, 1503 (1995).
[36]F. Iza, S. S. Yang, H. C. Kim, and J. K. Lee, J. Appl. Phys. **98**, 043302 (2005).
[37]D. W. Liu, F. Iza, and M. G. Kong, Plasma Processes Polym. **6**, 446 (2009).
[38]J. J. Shi and M. G. Kong, Appl. Phys. Lett. **87**, 201501 (2005).
[39]S. J. You, H. C. Kim, C. W. Chung, H. Y. Chang, and J. K. Lee, J. Appl. Phys. **94**, 7422 (2003).
[40]Kh. Tarnev, J. Engemann, and D. Korzec, Appl. Phys. Lett. **87**, 131504 (2005).
[41]D. W. Liu, F. Iza, and M. G. Kong, Appl. Phys. Lett. **93**, 261503 (2008).
[42]K. Shimizu, T. Ishii, and M. Blajan, IEEE Trans. Plasma Sci. **46**, 1125 (2010).
[43]M. Moravej, X. Yang, M. Barankin, J. Penelon, S. E. Babayan, and R. F. Hicks, Plasma Sources Sci. Technol. **15**, 204 (2006).
[44]E. J. Vera, M.S. thesis, Naval Postgraduate School, 1972.
[45]A. B. Callear and P. M. Wood, Trans. Faraday Soc. **67**, 272 (1971).
[46]K. Shimizu and T. Oda, Sci. Technol. Adv. Mater. **2**, 577 (2001).
[47]L. Gao, J. Sin, C. Feng, J. Bia, and H. Ding, Phys. Plasmas **19**, 013505 (2012).
[48]M. Laroussi and F. Leipold, Int. J. Mass. Spectrom. **233**, 81 (2004).
[49]G. C. Kim, H. W. Lee, J. H. Byun, J. Chung, Y. C. Jeon, and J. K. Lee, Plasma Processes Polym. **10**, 199 (2013).
[50]M. G. Kong, G. Kroesen, G. Morfill, T. Nosenko, T. Shimizu, J. V. Dijk, and J. L. Zimmermann, New J. Phys. **11**, 115012 (2009).
[51]H. Wk. Lee, H. W. Lee, S. K. Kang, H. Y. Kim, I. H. Won, S. M. Jeon, and J. K. Lee, Plasma Sources Sci. Technol. **22**, 055008 (2013).
[52]J. H. Choi, H. Wk. Lee, J. K. Lee, J. W. Hong, and G. C. Kim, Arch. Dermatol. Res. **305**, 133 (2013).